

Research papers

Gel-induced dew condensation

R. Urbina^{a,b}, S. Lefavrais^{a,c}, L. Royon^d, A. Mongruel^a, W. González-Viñas^b, D. Beysens^{a,c,*}^a Physique et Mécanique des Milieux Hétérogènes, UMR 7636 CNRS, ESPCI Paris - PSL University, Sorbonne Université, Sorbonne Paris Cité, 75005 Paris, France^b Universidad de Navarra, PHYSMED and Complex Systems Groups, Pamplona, Spain^c OPUR, 2 rue Verderet, 75016 Paris, France^d Laboratoire des Énergies de Demain, Sorbonne Paris Cité, UMR 8236 CNRS, 75013 Paris, France

ARTICLE INFO

Keywords:

Water harvesting

Hydrogel

Dew condensation

Vapor adsorption

ABSTRACT

Hydrogels are known to adsorb a large amount of vapor and liquid water, making them good candidates to enhance the amount of dew condensed from atmosphere. Although water vapor adsorption and liquid invasion in hydrogels have been the object of many studies, water condensation has been only little investigated. We address here the process of dew condensation on hydrogel grains widely used in agriculture (Aquasorb 3005TM). We show that dew condensing on hydrogels is enhanced when compared to a regular bare substrate due to vapor adsorption, which adds to condensation. Hydrogels, which can both capture water by vapor adsorption and condense water vapor with high efficiency, are thus good candidates to harvest water vapor from atmosphere with higher yield than regular bare surfaces.

1. Introduction

Hydrogels are three-dimensional networks of hydrophilic polymers, whose properties are known since more than 50 years (see e.g. Wichterle and Lim, 1960). There are many types of hydrogels (e.g. pH-, temperature-, electro- sensitive, light-responsive, etc.), with several applications related to their extraordinary swelling properties (volume can be multiplied by 1000) when immersed in liquid water (for a review, see e.g. Majee, 2016; Ganji et al., 2010). The osmotic pressure attributed to the polymer network is the driving force of swelling. An osmotic gradient indeed forms between the water solvent, low in ionic solute, towards the polymer, rich in ionic solute. The swelling process distends the network and is counterbalanced by the elastic contractility of the stretched polymer network. Due to this osmotic pressure, hydrogels can also exhibit high water adsorption from water vapor (they are hygroscopic), an adsorption which increases with relative humidity RH (see e.g. Delavoipière et al., 2018), making them suitable for atmospheric water harvesting (Zhao et al., 2019).

Water in hydrogels can be recovered by a moderate (~ 0.1 MPa) osmotic mechanical pressure (Milimouk et al., 2001; Zhang et al., 2017). The osmotic pressure exerted by plant roots in presence of soil water, on the order of 0.1–1.2 MPa, can be high enough to extract water from the gel mixed with soil and so provide water to the plant roots (Rudzinski et al., 2002; Puoci et al., 2008). For agriculture in arid and semi-arid

environments, there is an obvious interest to swell the gels with water obtained at the place where they need to be used, thus preventing water transportation on long distances. In consequence, collecting water from humid air by adsorption and/or dew condensation is very appealing.

The question we thus address in this study is whether, once exposed to humid air at night and cooled near or below the dew point, a typical hydrogel used in agriculture (Aquasorb 3005TM) could adsorb and/or condense more water than regular surfaces do. It appears that hydrogel can indeed condense water at a larger rate than a bare substrate. In addition, when gel temperature is above the dew point temperature, water adsorption still occurs.

The paper is organized as follows. After this introduction, details about the experiments and methods are given. Then the water adsorption process is investigated for relative humidity lower than 100%, followed by the study of condensation / adsorption at supersaturation larger than 1. The paper ends by some concluding remarks concerning the main results of the study.

2. Experiments and methods

The absorbent materials are samples of Aquasorb 3005TM, manufactured by SNF Floeger, a granular polyacrylamide. The materials are cross-linked copolymers of acrylamide and potassium acrylate, which are water insoluble and have a very high absorption capacity (ratio

* Corresponding author at: IPGP - Laboratoire PMMH, 1, rue Jussieu, 75005 Paris, France.

E-mail address: daniel.beysens@espci.fr (D. Beysens).

water weight/hydrogel weight up to 400). Further information can be found in Table 1 and from AquasorbTM 3005 (2020). The samples can be found in three sizes presentation (Dąbrowska and Lejcuś, 2012): small-size grains (diameter 0.19 ± 0.07 mm), medium-size grains (diameter 0.70 ± 0.2 mm) and large-size grains (diameter 1.5 ± 0.4 mm). Hereby we report results with small and medium grains.

The experimental apparatus is depicted in Fig. 1. It is placed inside a climatic chamber where air temperature and humidity are controlled. The setup consists of a cooling device, a silicon (Si) plate of diameter 10 cm and thickness 0.7 mm (condensing surface $S_c = 7.853 \times 10^{-3}$ m²), which holds the considered sample, and a balance to register the overall weight of sample and Si plate. The cooling device is held by a motorized support which moves it from an upper position, where it is in contact with the plate, to a lower position, where the plate is suspended by holders attached to the electronic balance and can be weighted. The Si plate is usually in contact with the cooling device. Each 30 s, the plate is moved to the lower position to be weighed, a step which lasts about 8 s. Temperature of the cooled plate is measured by calibrated thermocouples with an accuracy of 0.1 °C and a sensitivity of 0.01 °C. In the

Table 1

Some data on Aquasorb 3005TM gel (from Dąbrowska and Lejcuś, 2012; Aquasorb 3005, 2020).

Parameters	small size	medium size
Grain diameter (mm)	0.19 ± 0.07	0.70 ± 0.20
Specific weight (g.cm ⁻³)		1.1
Absorption capacity in 24 h (water mass/dry gel mass)	336	369

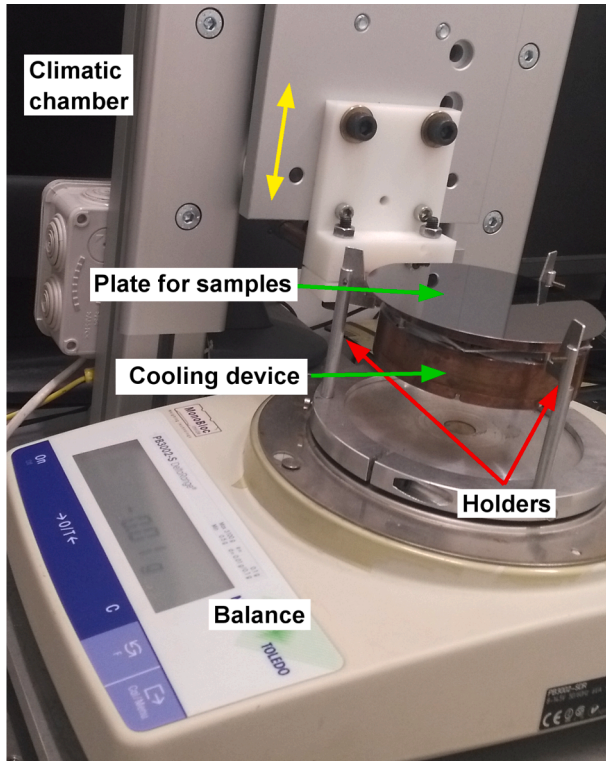


Fig. 1. Experimental setup in the climatic chamber. The sample is placed on a silicon plate cooled from below. The cooling device moves vertically (yellow double arrow). In the upper position, the cooling device is in contact with the plate and controls its temperature. In the lower position, the plate remains suspended from the holders fixed to the balance (red arrows) and the weight can be measured. A thermocouple is fixed below the plate to measure its temperature T_p . (For interpretation of the references to colour in this figure legend, the reader is referred to the web version of this article.)

chamber, air temperature T_a is set at 20 ± 0.5 °C and relative humidity at $50 \pm 3\%$, which corresponds to a vapor pressure of 1.15 kPa and a dew point temperature $T_d = 9.3 \pm 0.1$ °C.

The gel sample grains are poured on the silicon plate by the help of a circular mold which keeps the sample height < 1 mm to form a thin layer. In order to have identical departure conditions in all cases, all the samples were previously dried at 40 °C during 8 h and stored in a closed box with silica gel to maintain a low humidity level. For each experiment, the conditions inside the chamber and the cooling device temperature are fixed at their desired value before placing the plate with the gel.

Two different conditions were investigated, above or below the dew point, which corresponds to either relative humidity $RH \leq 100\%$ (above the dew point) or supersaturation $SR > 1$ (below the dew point). Relative humidity and supersaturation are defined from water vapor pressures as

$$SR \text{ or } RH \left/ 100 = \frac{p(T_a)}{p_s(T_p)} \quad (1)$$

Here, $p(T_a)$ is the water vapor pressure in the air surrounding the plate and $p_s(T_p)$ is the water vapor saturation pressure at substrate (plate) temperature. In addition to the determination of characteristic adsorption isotherms under various RH , typical temperature conditions as encountered at night outdoors were specially investigated: (i) Above the dew point with a plate temperature $T_p = T_d + 4$ K (adsorption), (ii) below the dew point : $T_p = T_d - 4$ K.

3. Above the dew point

The dynamics of adsorption is classically governed by two processes (see e.g. Ganji et al., 2010). One process is water molecules diffusing in the gel by Fick's law due to the difference of water concentration between humid air (c_0 , corresponding to water vapor pressure $p \sim RH$) and water concentration in gel (c_c). The other process is the stretching relaxation of the polymer chains.

For typical times corresponding to adsorption amplitudes lower than 60% of the limiting saturation value, the adsorption data measured by $\omega_i = m_w/m_i$ (m corresponds to mass with subscript w for water and subscript $i = s$ or m for dry small and medium size gel grains) can be fitted to the power law revealing the mode of relaxation:

$$\omega_i = m_w/m_i = A_i t^x \quad (2)$$

A_i is an amplitude and x an exponent whose value corresponds to the gel relaxation process. For pure Fickian diffusion, $x = 1/2$. For pure gel relaxation, $x = 1$. In general, the exponent is between 1/2 and 1, corresponding to both relaxation-controlled transport and diffusion-controlled processes. Equation (2) can thus be generalized. With A_i, B_i corresponding to amplitudes related to the two processes:

$$\omega_i = A_i t^{1/2} + B_i t \quad (3)$$

For adsorption amplitudes larger than 60% of the limiting saturation value, the approach to saturation can be described in the case of diffusion by the Fick's law. For a spherical particle of radius R , initial radius R and surface $S = 4\pi R^2$ one obtains, neglecting the radius change in the concentration gradient as swelling remains small in the adsorption process:

$$\frac{1}{S} \frac{dm_w}{dt} = -D_p \nabla c = D_p \frac{c_0 - c_c}{R} \sim D_p \frac{c_0 - c_c}{R_i} \quad (4)$$

where D_p is the water diffusion coefficient in the polymer.

The adsorbed mass corresponds to water concentration in the gel, $c_c = 3m_w/(4\pi R_i^3)$. The solution to this equation leads to the following exponential decay evolution, in terms of ratio ω_i :

$$\omega_i = \omega_{i,\infty} (1 - e^{-t/\tau_i}) \quad (5)$$

Here $\omega_{i,\infty}$ is the maximum rate of water in the saturated gel,

$$\omega_{i,\infty} = \frac{4\pi R_i^3 c_0}{3m_i} \propto RH \quad (6)$$

and the typical relaxation time, τ_i , reads as

$$\tau_i = \frac{R_i^2}{3D_p} \quad (7)$$

Since the diffusion of vapor around the grains limits the process (as in the case of thin film studies by Delavoipière et al. (2018)), the adsorption dynamics depends on the thickness of the diffuse boundary layer, that is the layer where a Peclet number $Pe = \frac{UL}{D} < 1$. Here, U is the air flow velocity far from the substrate, L is the characteristic length of the substrate and D is the diffusivity of water molecules in air. In our study, the hydrodynamic conditions are the same for all studied substrates, small or medium grains, and difference in kinetics can be only attributed to RH and the grain size.

In the case where the gel relaxation dominates the process, a relation similar to Eq. (5) is found, however with a relaxation time which is independent of gel grain radius and relates to the relaxation of the gel network,

$$\omega_i = \omega_{i,\infty} (1 - e^{-t/\tau_i}) \quad (8)$$

with $\tau_i = \text{const.}$

The evolution due to diffusion plus gel relaxation can thus be written as:

$$\omega_i = \omega_{i,\infty} (1 - e^{-t/\tau_i}) + \omega_{i,\infty} (1 - e^{-t/\tau_i}) \quad (9)$$

In Fig. 2 are reported typical adsorption isotherms and in Table 2 the results of the fits to Eqs. (2) and (3) using data in the range $\omega_i < 0.6\omega_{i,\infty}$. For small grains, the exponent of single power law, Eq. (2), are found in the range [0.58 – 0.79], with mean value 0.69 closer to 0.5 than to 1, showing that vapor diffusion plays the major role in the relaxation process. This is corroborated with double power law fit, Eq. (3), where the amplitude of the $t^{1/2}$ term is about 10 times larger than the t term. For medium grains, the relaxation is too long to obtain data close to saturation, then the fit to exponential decay Eq. (5) is made over all the data range, which gives an estimation of $\omega_{m,\infty}$. Data are then fitted to power laws in the range $\omega_m < 0.6\omega_{m,\infty}$.

The results of the fit to the exponential relaxation, Eq. (5), are reported in Table 2. According to Eq. (5), the ratio of relaxation times $\tau_m/\tau_s \approx (R_m/R_s)^2 \approx 13.6$. The measured ratio is smaller, $\tau_m/\tau_s \approx 4.88$, confirming that gel relaxation also matters. Considering only water

diffusion in the polymer, one infers $D_p \sim 10^{-11} \text{ m}^2 \cdot \text{s}^{-1}$, a typical value in gels.

Data (Fig. 2a) show, as expected (see e.g. Delavoipière et al., 2018), that RH is the only parameter for the adsorption amplitude $\omega_{i,\infty}$ (see the isotherms at $T_a = T_p = T_d + 11 \text{ K}$ and $T_d + 4 \text{ K}$ with air at same temperature than the substrate and $RH = 78\%$). Adsorption where the plate temperature is at a temperature lower than air ($T_p = T_d + 4 \text{ K}$, air at $T_a = 20^\circ \text{C}$ and $RH = 50\%$) would correspond to a mean isotherm at $RH \approx 64\%$. Medium grains isotherms (Fig. 2b) correspond to the last case ($T_p = T_d + 4 \text{ K}$, air at $T_a = 20^\circ \text{C}$ and $RH = 50\%$).

4. Below the dew point

When the substrate temperature is set below the dew point temperature, condensation takes place. Condensation on gels exhibits specific features when compared with condensation on a bare surface.

4.1. Region of inhibited condensation.

In Fig. 3 is shown thin ($< 1 \text{ mm}$) layers of small and medium gel grains in a circle of radius $R_g \sim 15 \text{ mm}$ on a bare Si surface at $T_p = T_d - 6.7 \text{ K}$. Dropwise condensation is observed on the Si surface naturally coated with an oxidation layer whose contact angle with water is $\theta \approx 60^\circ$ (see e.g. Narhe and Beysens, 2004).

The hygroscopic nature of the gel due to the osmotic pressure built-up by its hydrophilic sites induces enhanced adsorption of water vapor and thus lowers vapor pressure at the gel border, giving rise to a region of inhibited condensation (RIC) on the bare silicon substrate surrounding the gel sample, with width δ^* as defined in Fig. 3. This RIC is similar to the dry region around lyophilic patches during diethylene glycol condensation (Schäfle et al., 2003 or around a salty droplet (Guadarrama-Cetina et al., 2014).

To obtain the δ^* and R_g values shown in Fig. 4, the processing of the images includes smoothing, contrast enhancement and border detection, which was performed by using the Fiji® routines. Due to the irregular borders (see Fig. 3), the average distance between the gel and the condensation pattern was determined within a small region.

Fig. 4 reports the evolution of the RIC width δ^* , which decreases with time. This RIC decrease can be attributed to the increasing impregnation of the gel with adsorbed water. When the gel is saturated, condensation on gel proceeds with the same way as on the bare substrate, as seen in Section 4.2. The RIC width should be at that time the same as the RIC observed around each water drops or hydrophilic dots (corresponding to the lyophilic patches of Schäfle et al., 2003), as a result of the surrounding water vapor gradient (see e.g. Beysens, 2018). The mechanism

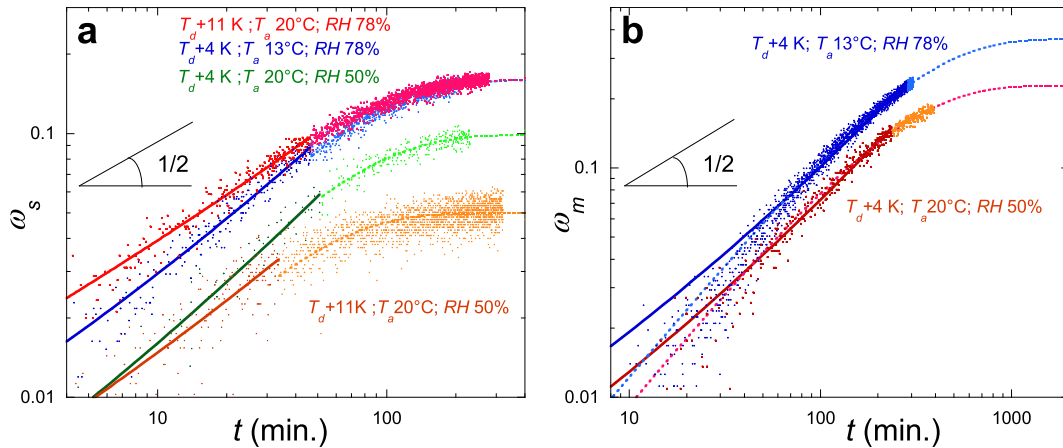
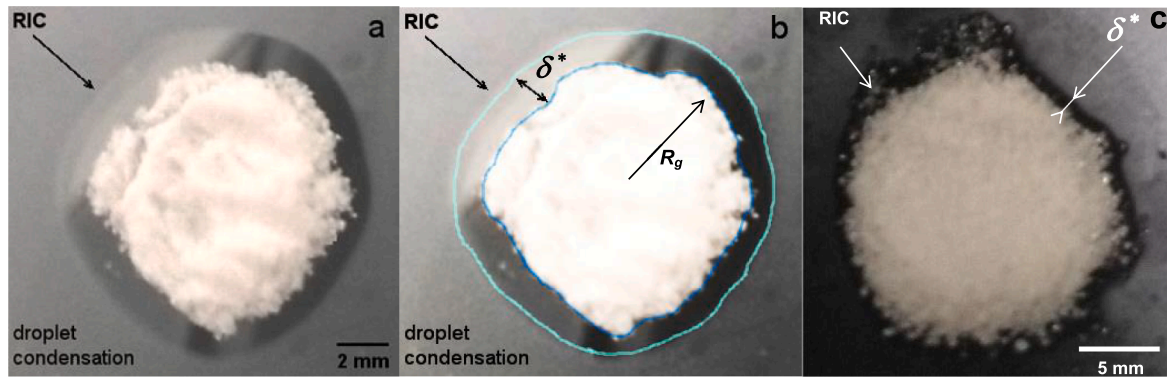
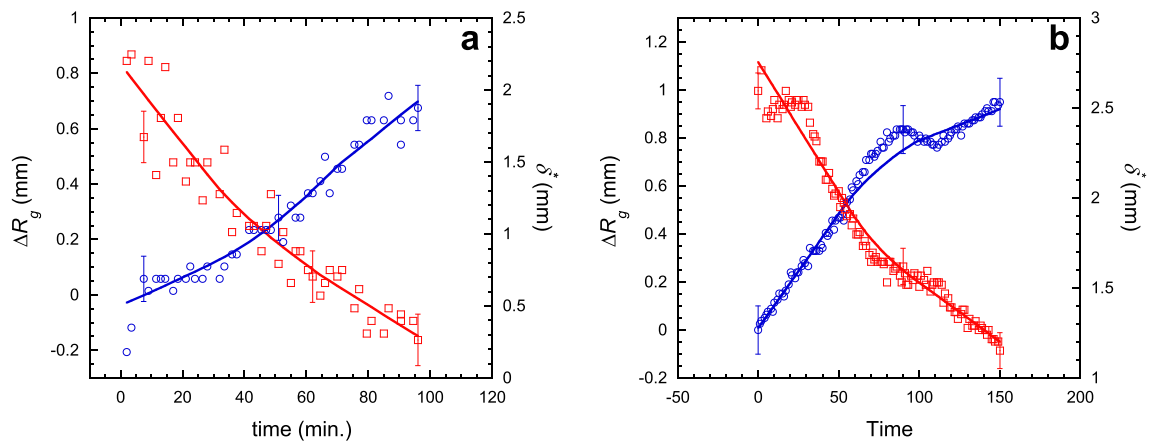


Fig. 2. Evolution of sorption isotherms ($\omega_{i-s,m}$, log-log plot, $RH < 100\%$). The full straight lines are power law fits to data 60% below the saturation value (Eq. (2)) and the interrupted curves are exponential fits to data above 60% of the saturation value (Eq. (5)) (see Table 2). (a) Small grains. (b) Medium grains, where exponential fit is made with all data (see text).

Table 2

Results of the fits of the adsorption data. Uncertainties: One standard deviation.

Fitting	Parameter	Small grains			Medium grains			Bare	
Single power law Eq. (2)	RH (%)	50	≈ 64	78	≈ 64	78	SR	1.32	
	$T_p - T_d$ (K)	11	4	4	11	4			
	m_i (g)	9.75	9.14	9.20	9.00	7.34			
	A_i	$0.0032 \pm 4 \times 10^{-4}$	$0.0026 \pm 4 \times 10^{-4}$	$0.0056 \pm 2 \times 10^{-4}$	$0.0102 \pm 2 \times 10^{-4}$	$0.0169 \pm 8 \times 10^{-5}$	$0.00257 \pm 5 \times 10^{-5}$		
	x	0.66 ± 0.03	0.79 ± 0.04	0.72 ± 0.01	0.58 ± 0.01	0.81 ± 0.03	0.80 ± 0.03		
Double power law Eq. (3)	A_i	$0.0034 \pm 4 \times 10^{-4}$	$0.0026 \pm 6 \times 10^{-4}$	$0.00608 \pm 3 \times 10^{-4}$	$0.0109 \pm 2 \times 10^{-4}$	$0.004238 \pm 6 \times 10^{-6}$	$0.0026 \pm 2 \times 10^{-4}$		
	B_i	$0.00040 \pm 8 \times 10^{-5}$	$0.0008 \pm 1 \times 10^{-4}$	$0.00102 \pm 5 \times 10^{-5}$	$0.0048 \pm 4 \times 10^{-5}$	$0.000586 \pm 9 \times 10^{-5}$	$0.00046324 \pm 1 \times 10^{-5}$		
Exponential decay Eq. (5)	$\omega_{i,\infty}$	$0.0499 \pm 1 \times 10^{-4}$	$0.0989 \pm 7 \times 10^{-4}$	$0.1593 \pm 5 \times 10^{-4}$	$0.1592 \pm 3 \times 10^{-4}$	$0.228 \pm 2 \times 10^{-3}$	$0.365 \pm 3 \times 10^{-3}$		
	τ_i (min.)	39 ± 0.6	60 ± 1.5	64.8 ± 0.6	55.8 ± 0.4	242 ± 2	294 ± 3		
Lin. evol. Eq. (11)	dh/dt ($\times 10^{-3}$ mm. min. $^{-1}$)							$1.4207 \pm 2 \times 10^{-3}$	

**Fig. 3.** Examples of region of inhibited condensation (RIC) around a thin (<1 mm) layer of (a, b) small size grain at $t = 25$ s. (b) is the (a) picture with outlined gel and RIC contours. (c) Medium size grains, $t = 25$ s. ($T_d = 22$ °C at 47% RH, $T_p = T_d - 6.7$ K).**Fig. 4.** Evolution of the RIC width δ^* (squares) and gel radius increase ΔR_g (circles) as observed in Fig. 3 of (a) small grains and (b) medium grains. The curves are data smoothing. ($T_d = 20$ °C, $RH = 50\%$, $T_p = T_d - 4$ K).

behind the RIC evolution is thus different to what happens with a solute sample (e.g. a salty drop as in [Guadarrama-Cetina et al., 2014](#)), which comes from a reduction of saturation pressure (Raoult law) or around an ice crystal where the constant drop in saturation pressure makes the RIC width constant ([Nath et al., 2018](#)). (Further analysis is out of the scope of the present study).

The evolution of the gel radius increase, $\Delta R_g = R_g(t) - R_g(0)$, is shown in Fig. 4. The ΔR_g growth rate decreases after about a time ~ 100

s for medium grains, a value near the time where the condensation rate exhibits an inflection corresponding to the lowest influence of the adsorption process (see Fig. 5). The ΔR_g increase is due to both adsorption and condensation processes and is proportional to the collected increasing water volume per unit surface, h , (see Eq. (11)). The prefactor is, however, difficult to precisely evaluate because it depends on the grains packing. It is clear in Fig. 4b that the rate of growth is larger at early times, as in Fig. 5. Note that the ΔR_g behavior can be affected by

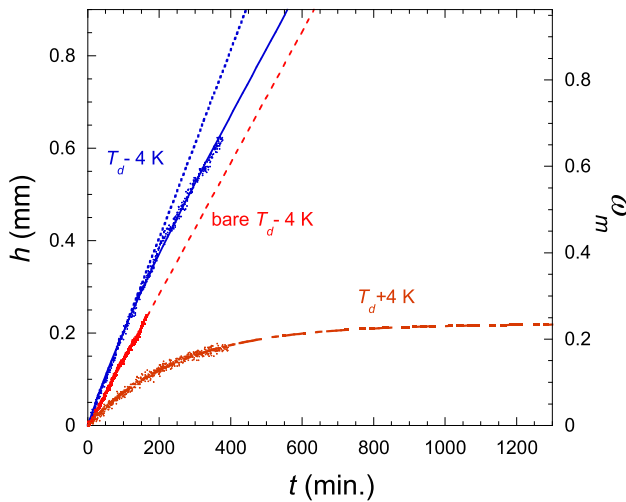


Fig. 5. Evolution of condensation ($SR = 1.32$) on gel medium grains (blue dots) and bare substrate (red dots) under same conditions ($T_d = 20^\circ\text{C}$, $RH = 50\%$, $T_p = T_d - 4\text{ K}$). Left ordinate: water volume per unit projected area, h . The continuous curve is a fit of gel data to Eq. (12) and the interrupted line is a fit of bare substrate to Eq. (11). The dotted line is the initial slope for condensation on gel. For the sake of comparison, the sorption isotherm at $T_d = 20^\circ\text{C}$, $RH = 50\%$, $T_p = T_d + 4\text{ K}$ is also reported (orange dots; right ordinate; see Fig. 2b). (For interpretation of the references to colour in this figure legend, the reader is referred to the web version of this article.)

the grains rearrangement during their swelling, which presumably explains the different behavior between small and medium grains and the oscillations in the R_g evolution as observed in Fig. 4b.

4.2. Condensation rates

In order to compare the adsorption volume with respect to condensation on a bare substrate, one considers the surfacic adsorbed volume or equivalent water film thickness, h . With ρ the water density, this layer is expected to grow proportionally to time as

$$h = \frac{m_w}{\rho S_c} t \quad (11)$$

In Fig. 5 is reported condensation on gels and bare substrate. The bare substrate condensation is proportional to time with slope $(dh/dt)_b = 1.4207 \times 10^{-3} \pm 2 \times 10^{-6} \text{ mm} \cdot \text{min}^{-1}$ (uncertainty: 1 SD). Gel exhibits a larger initial rate up to time ≈ 100 min. where the rate progressively decreases to reach the bare substrate value, corresponding to condensation and imbibition of the gel as if it were a bare substrate. The swelling ratio at which this inflection occurs (~ 0.2) is far less than the maximum swelling ratio of ~ 370 and cannot be attributed to the vicinity of this limit. One notes that further to this inflection the slope becomes comparable to what is found on the bare surface. This rate decrease towards the bare substrate value can be related to the corresponding decrease of the RIC width and decrease of the rate of gel radius growth, ΔR_g , which occurs during the same time period, and which corresponds to the approach of the saturation of adsorption. In order to assess this point, the gel data have been fitted to the sum of condensation as if the gel were a bare substrate, Eq. (11) and the adsorption evolution, in volume per unit surface as in Eq. (5):

$$h = \left(\frac{dh}{dt} \right)_b t + h_{m,\infty} (1 - e^{-t/\tau_m}) \quad (12)$$

From Table 2, the amplitude value of the adsorption data at $T_d + 4\text{ K}$ can be expressed in volume per projected gel surface area, $h_{m,\infty} = \omega_{i,\infty} m_i / S_c = (0.201 \pm 0.002) \text{ mm}$. Gel condensation data are fitted to Eq. (12) with $(dh/dt)_b$ free and imposed. The results are listed in Table 3. When all parameters are left free, $(dh/dt)_b$ is found somewhat smaller

Table 3

Results of the fit to Eq. (11) of condensation data on gel (Fig. 5). The values under brackets are imposed in the fit. The gel mass is $m_m = 6.94\text{ g}$. Notations: see text.

$(dh/dt)_b \text{ (mm} \cdot \text{min}^{-1})$	$h_{m,\infty} \text{ (mm)}$	$\tau_m \text{ (min.)}$	χ^2
0.070	$(1.1 \pm 0.1) \times 10^{-3}$	0.24 ± 0.05	195 ± 31
0.054	(1.4207×10^{-3})	0.106 ± 0.001	115 ± 4
0.082	(1.4207×10^{-3})	0.165 ± 0.001	(300)
0.15	(1.4207×10^{-3})	(0.201)	391 ± 5

than on the bare substrate, presumably because of the lack of data at very long times. The adsorption time is found somewhat lower (195 s) than at $T_d + 4\text{ K}$ (300 s). The amplitude (0.24 mm) compares relatively well with what is expected (0.201 mm). With $(dh/dt)_b$ imposed, the typical adsorption time is 3 time smaller than expected and the adsorption amplitude is too small (0.106 mm). When the adsorption time is fixed at the value at $T_d + 4\text{ K}$ (300 s), the amplitude (0.165 mm) increases but still remains smaller than the value at $T_d + 4\text{ K}$. With the latter amplitude imposed at 0.201 mm the adsorption time (391 s) becomes closer to the time at $T_d + 4\text{ K}$ (300 s), with however a χ^2 somewhat larger than the two previous fits (A more detailed analysis would need more data and is out of the scope of the present study.).

It thus results a net increase of water absorbed on gel when compared to the bare substrate under same conditions, with value on the order of 0.1 mm. This behavior can be explained by the fact that two phenomena are present: (i) an initial adsorption of water vapor, giving a vapor concentration gradient above the surface of the gel larger than on the bare substrate, at the origin of a RIC, followed by (ii) a steady condensation with the same concentration gradient as found above the water drops on the bare substrate. Water will continue to condense on the gel until it reaches its maximum swelling. As a result of the initial large water absorption rate, water absorbed by the gel is thus found in greater amount than water condensed on the bare plate.

Note that if instead of gel particles, one considers a gel film, one should obtain similar enhancement as the adsorption phenomenon is not due to the macroscopic shape of the gel but to the intrinsic properties of the polymer network. A gel film will then equally serve to condense water vapor and the swelling mechanism due to adsorption plus condensation will be the same. The only difference would be the value of the exposed area to condensation, which is smaller, then the condensation rate will be lower. The maximum swelling volume capacity, proportional to the gel volume, will also be smaller. As a matter of fact, such gel film condensation has already been reported by Delavoipière et al., 2018. On the other hand, if there were any non-water vapor absorbing hydrophilic powder on the surface instead of the gel particles, one would simply expect no adsorption. Only filmwise condensation will occur (coefficient $h_{m,\infty} = 0$ in Eq. (12)).

5. Concluding remarks

Common hydrogels grains used for soil in agriculture (Aquasorb 3005TM) can collect water even for relative humidity $< 100\%$. They also exhibit interesting properties when used in supersaturation conditions (conditions of dew formation) since they collect more water than a bare hydrophobic substrate with same projected surface area. The measured gain is on order 0.1 mm of water / day, which is an important gain when compared to the current values found for dew yield (0.1–0.6 mm/day). This enhanced condensation of water is due to the initial water vapor adsorption, which adds to condensation. As noted in the introduction, such condensed water stored in gels can be either used in agriculture where the osmotic pressure exerted by the roots is sufficiently high to extract water or removed by moderate (~ 1 bar) mechanical pressure for human use (Milimouk et al., 2001). Another way is to evaporate water and condense it in e.g. a solar still (see e.g. Zhao et al., 2019 where details on needed energy and time duration are given). Although the use

is one and only in agriculture where the grains are definitely mixed with the soil, water extraction by pressure or evaporation has to be cyclically repeated. There is, however, a possible limitation to the number of cycles due to the absorption of CO₂ gas from the atmosphere. HCO₃⁻ ions are indeed added in the solutions, screening the polymer charges and thus progressively reducing the swelling amplitude (see e.g. Ríčka and Tanaka, 1984 for ions influence). Precise evaluations remain to be carried out.

In addition, although the above study has been performed in laboratory by contact cooling, preliminary experiments under outdoor radiative cooling (Beysens, 1998) give, at least qualitatively, the same results. Emissivity of dry gels is indeed high, as in any organic materials and, when wet, their emissivity becomes close to pure water emissivity (0.98; Schott et al., 2001). Outdoor radiative condensation unsurprisingly exhibits the same properties and constraints than condensation on a solid substrate (e.g. clear sky, high nocturnal relative humidity, low wind speed, water evaporation under direct sun light; see Beysens, 2018). Further research will be needed to get a Proof of Concept, but these results are already very encouraging in view of the development of new materials to enhance dew water collection.

CRediT authorship contribution statement

R. Urbina: Investigation, Formal analysis, Data curation, Writing - review & editing. **S. Lefavrais:** Methodology, Resources, Writing - review & editing. **L. Royon:** Software, Methodology, Visualization, Writing - review & editing. **A. Mongruel:** Project administration, Investigation, Visualization, Funding acquisition, Supervision, Writing - review & editing. **W. González-Viñas:** Software, Validation, Funding acquisition, Supervision, Writing - review & editing. **D. Beysens:** Conceptualization, Methodology, Project administration, Data curation, Formal analysis, Supervision, Writing - original draft, Writing - review & editing.

Declaration of Competing Interest

The authors declare that they have no known competing financial interests or personal relationships that could have appeared to influence the work reported in this paper.

Acknowledgments

We gratefully thank E. Verneuil for discussions. R.U. acknowledges a

financial support from the “Asociación de Amigos de la Universidad de Navarra”. This work was partially supported by the Spanish AEI (Grants FIS2014-54101-P and FIS2017-83401-P).

References

- AquasorbTM 3005, 2020. https://snf.com.au/downloads/Aquasorb_E.pdf.
- Beysens, D., 1998. Outdoor water adsorption and condensation on a polyelectrolyte gel. CEA Internal report.
- Beysens, D., 2018. *Dew Water*. Rivers Publisher, Gistrup.
- Dąbrowska, J., Lejcuś, K., 2012. Characteristics of selected properties of superabsorbents. *Polska Akademia Nauk* 3/IV, 59–68. (In Polish).
- Delavoipière, J., Heurtefeu, B., Teisseire, J., Chateauminois, A., Tran, Y., Fermigier, M., Verneuil, E., 2018. Swelling dynamics of surface-attached hydrogel thin films in vapor flows. *Langmuir* 34 (50), 15238–15244.
- Ganji, F., Vasheghani-Farahani, S., Vasheghani-Farahani, E., 2010. Theoretical description of hydrogel swelling: a review. *Iran. Polym. J. (English)* 5, 375–398.
- Guadarrama-Cetina, J., Narhe, R.D., Beysens, D.A., González-Viñas, W., 2014. Droplet pattern and condensation gradient around a humidity sink. *Phys. Rev. E* 89 (1). <https://doi.org/10.1103/PhysRevE.89.012402>.
- Majee, S.B. (Ed.), 2016. *Emerging concepts in analysis and applications of hydrogels*, Intech, Rijeka.
- Milimouk, I., Hecht, A.M., Beysens, D., Geissler, E., 2001. Swelling of neutralized polyelectrolyte gels. *Polymer* 42 (2), 487–494.
- Narhe, R.D., Beysens, D.A., 2004. Nucleation and growth on a superhydrophobic grooved surface. *Phys. Rev. Lett.* 93 (7) <https://doi.org/10.1103/PhysRevLett.93.076103>.
- Nath, Saurabh, Bisbano, Caitlin E., Yue, Pengtao, Boreyko, Jonathan B., 2018. Duelling dry zones around hygroscopic droplets. *J. Fluid Mech.* 853, 601–620.
- Puoci, Francesco, Iemma, Francesca, Spizzirri, Umile Gianfranco, Cirillo, Giuseppe, Curcio, Manuela, Picci, Nevio, 2008. Polymer in agriculture: a review. *Am. J. Agric. Biol. Sci.* 3 (1), 299–314.
- Ríčka, J., Tanaka, T., 1984. Swelling of Ionic Gels: Quantitative Performance of the Donnan Theory. *Macromolecules* 17, 2916–2921.
- Rudzinski, W.E., Dave, A.M., Vaishnav, U.H., Kumbar, S.G., Kulkarni, A.R., Aminabhavi, T.M., 2002. Hydrogels as controlled release devices in agriculture: review. *Des. Monomers Polym.* 5, 39–65.
- Schäfle, C., Leiderer, P., Bechinger, C., 2003. Subpattern formation during condensation processes on structured substrates. *Europhys. Lett.* 63 (3), 394–400.
- Schott, John R, Barsi, Julia A, Nordgren, Bryce L, Raqueno, Nina Gibson, de Alwis, Dilkushi, 2001. Calibration of Landsat thermal data and application to water resource studies. *Remote Sens. Environ.* 78 (1–2), 108–117.
- Wichterle, O., Lím, D., 1960. Hydrophilic gels for biological use. *Nature* 185 (4706), 117–118.
- Zhang, Y.R., Tang, L.Q., Xie, B.X., Xu, K.J., Liu, Z.J., Liu, Y.P., Jiang, Z.Y., Dong, S.B., 2017. A variable mass meso-model for the mechanical and water-expelled behaviors of PVA hydrogel in compression. *Int. J. Appl. Mech.* 09 (03), 1750044. <https://doi.org/10.1142/S1758825117500442>.
- Zhao, Fei, Zhou, Xingyi, Liu, Yi, Shi, Ye, Dai, Yafei, Yu, Guihua, 2019. Super moisture-absorbent gels for all-weather atmospheric water harvesting. *Adv. Mater.* 31 (10), 1806446. <https://doi.org/10.1002/adma.v31.1010.1002/adma.201806446>.